# Main group metal halide complexes with sterically hindered thioureas
# XII. Crystallographic studies of lead(II) and cadmium(II) thiocyanate complexes with 1,3-dimethyl-2(3*H*)-imidazolethione

Daniel J. Williams*
*Department of Chemistry and Physics, Kennesaw State College, Marietta, GA 30061 (USA)*

Donald VanDerveer, Leigh Ann Lipscomb
*School of Chemistry, Georgia Institute of Technology, Atlanta, GA 30332 (USA)*

and Robert L. Jones
*Department of Chemistry, Emory University, Atlanta, GA 30322 (USA)*

(Received August 8, 1991)

**Abstract**

The complex, $Pb(NCS)_2(dmit)_2$, has been previously reported (dmit = 1,3-dimethyl-2(3*H*)-imidazolethione). A new complex, $Cd(NCS)_2(dmit)_2$, has also been synthesized and characterized. Single crystal X-ray structural studies were completed for both complexes. Cell parameters for $[Pb(NCS)_2(dmit)_2]$: space group *C2/c*, $a = 11.118(2)$, $b = 14.121(4)$, $c = 12.970(3)$ Å, $\beta = 108.29(2)°$, $Z = 4$, $V = 1933.4$ Å$^3$, $D_c = 1.895$ g/cm$^3$, $D_0 = 1.93$ g/cm$^3$ ($\lambda = 0.71073$ Å), $R = 0.030$; $[Cd(NCS)_2(dmit)_2]$: space group *C2/c*, $a = 10.911(2)$, $b = 14.172(2)$, $c = 12.471(2)$ Å, $\beta = 107.54(1)°$, $Z = 4$, $V = 1838.7$ Å$^3$, $D_c = 1.752$ g/cm$^3$, $D_0 = 1.75$ g/cm$^3$ ($\lambda = 0.71073$ Å), $R = 0.031$. Both complexes are isostructural polymers comprised of zigzag chains of $MS_4N_2$ distorted octahedra sharing common edges through almost perfectly linear bridging SCN groups displaced *cis* to each other relative to the central metal atom. Thiourea ligands are displaced *trans* to each other. Comparative bond distances show the formulation of these complexes to be more accurately stated as $M(NCS)_2(dmit)_2$. There is no clear evidence for the lone pair of electrons through systematic distortions in the lead structure although there are greater observed deviations from 90° in the local site symmetry about Pb than about Cd.

## Introduction

In Part VIII of this series [1] we reported the synthesis and characterization of $Pb(NCS)_2(dmit)_2$ (dmit = 1,3-dimethyl-2(3H)-imidazolethione, Fig. 1(a)) in which we predicted a bridged polymeric structure with possible N-bonded formulation. This prediction was based primarily on comparison of observed solid state vibrational data for the SCN group with reported spectra for thiocyanate complexes of known structures such as $Pb(NCS)_2$ [2] and $Pb(NCS)_2(dmso)_2$ (dmso = dimethyl sulfoxide) [3]. The observed high melting point and low solubility in most common solvents gave further support to this speculation. We have recently determined the structure of $Pb(NCS)_2(dmit)_2$ via X-ray crystallography and have synthesized a new complex, $Cd(NCS)_2(dmit)_2$, which we have also characterized by X-ray structural methods. An earlier paper by Calvaca *et al.* [4] reported the crystal structures for $Cd(NCS)_2(etu)_2$ and $Pb(NCS)_2(etu)_2$ (etu = ethylenethiourea, Fig. 1(b)) which were observed to be isomorphous. A detailed crystallographic study was completed for $Cd(NCS)_2(etu)_2$ only, however, and based on the isomorphic relationship, the lead complex was assumed to be isostructural. A more recent example of isostructural correlation with isomorphic crystalline

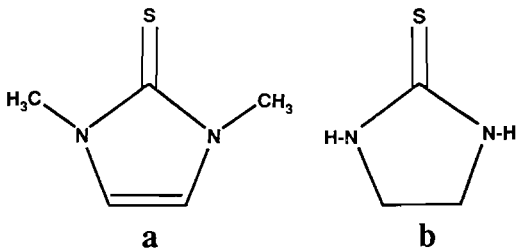


a b

Fig. 1. (a) 1,3-Dimethyl-2(3*H*)-imidazolethione (dmit); (b) ethylenethiourea (etu).

*Author to whom correspondence should be addressed.

0020-1693/92/$5.00

habits is seen in a study detailing the structures of polymeric mono-oxalato complexes of Cd(II) and Pb(II) [5]. The structure of $Cd(NCS)_2(etu)_2$ was observed to be made up of polymeric zigzag chains of $Cd(NCS)_4(etu)_2$ octahedra linked by bridging SCN groups. The N-bonded configuration was determined based on comparative bond distances.

Our initial interest in the structure of $Pb(NCS)_2(dmit)_2$ was to determine if it indeed were polymeric and if it had any similarity to the structure reported for $Cd(NCS)_2(etu)_2$. If the lead atom were hexa-coordinated, $Pb(NCS)_2(dmit)_2$ would be an $AX_6E$ complex (A = central atom, X = ligand, E = non-bonded electron lone pair) thus making the stereoactivity of the lone pair a major question. For this reason, the Cd(II) analog was synthesized and characterized since comparison between $Cd(NCS)_2(dmit)_2$ and $Cd(NCS)_2(etu)_2$ structures could provide significant insight interpreting the Pb(II) data if $Pb(NCS)_2(dmit)_2$ were found to be isostructural. Not only would such a comparison allow ligand-induced structural differences to be sorted from repulsion effects brought on by the lone pair of electrons in the Pb(II) complex, but it would be helpful to note if there were any radical differences such as the one noted in one of our earlier studies [6] between the structures of $BiCl_3(dmit)_2$ and $BiCl_3(etu)_2$ reported by Battaglia *et al.* [7].

The following paper details the results of crystal structures for $Pb(NCS)_2(dmit)_2$ and $Cd(NCS)_2(dmit)_2$ as well as the synthesis and characterization of the latter. Solution state data and upgraded solid state vibrational data which include Fourier transform infrared and laser Raman (FT-IR and FT-Raman) spectra are also presented and discussed for these two complexes.

## Experimental

### *Chemicals*

All chemicals were reagent grade and used as commercially obtained without further purification. Spectroscopic grade $CD_3CN$ (Aldrich) was used as a solvent to obtain the proton NMR data. Electrical grade anhydrous $CH_3CN$ (Fisher) was used as obtained without further purification for specific conductivity measurements (L = 6 $\mu$mhos). Dmit was synthesized as previously reported [8].

### *Analytical*

Carbon, hydrogen and nitrogen analyses were done by Atlantic Microlabs, Inc.

### *Solution studies*

Specific conductivity for $Cd(NCS)_2(dmit)_2$ was measured in $CH_3CN$ using methods previously reported [1]. Proton NMR were recorded in $CD_3CN$ on a 300 MHz GE model QE-300 FT-NMR spectrometer. Chemical shifts are reported in ppm ($\delta$) relative to external tetramethylsilane (key: s = singlet, d = doublet.)

### *Solid state spectra*

IR spectra were recorded as mineral oil (Nujol) mulls between AgCl plates from 4000 to 400 $cm^{-1}$ on a Mattson Galaxy 2020 FT-IR spectrophotometer. Raman data were collected on powders from 4000 $cm^{-1}$ to excitation line using a Bruker IFS-66 FT-Raman spectrophotometer equipped with Nd-YAG laser ($\lambda_{ex} = 1.063$ $\mu$m). Only the peaks within the range of primary interest (viz. up to 2100 $cm^{-1}$) are reported below. All values are reported in $cm^{-1}$ ($\pm 4$) (key:v = very, w = weak, m = medium, s = strong, br = broad, sh = shoulder).

### *Synthesis*

Melting points (uncorrected) were obtained on a Fisher-Johns stage-type apparatus and reported in degrees Celsius. The synthesis and characterization of $Pb(NCS)_2(dmit)_2$ has already been reported [1], but the hitherto unreported Raman data as well as the FT-IR data are reported below. Crystallographic grade crystals were grown from hot water.

#### *Bis[1,3-dimethyl-2(3H)-imidazolethione]di-N-thiocyanatocadmium(II)*

In a flask placed on a hot plate equipped with magnetic stirrer were placed 5.0 g $Cd(NO_3)_2 \cdot 5H_2O$ (16 mmol), 3.0 g $NH_4SCN$ (39 mmol), 3.0 g NaSCN (37 mmol), and *c.* 75 ml $H_2O$. To this solution was added 8.0 g dmit (64 mmol) in 25 ml ethanol (95%) with stirring. A white powder formed with mild heating and stirring. The product was filtered and washed with small portions of 95% ethanol. A nearly quantitative yield of 7.0 g was obtained. Large clear white crystallographic grade crystals were obtained by evaporation from acetonitrile. m.p. 109–111 °C. *Anal.* Calc. for $C_{12}H_{16}N_4S_4Cd$: C, 29.72; H, 3.33; N, 17.33. Found: C, 29.70; H, 3.33; N, 17.37%. $\Lambda_M$ (*c.* $10^{-3}$ M in $CH_3CN$) = 22.6 mho $cm^2$/mol. Proton NMR($\delta$): 3.53 (s, 3H, methyl), 6.94 (s, 1H, ethylenic). IR (Nujol mull): 2086s,br, 1666m, 1565s, 1346s,sh, 1315m,sh, 1255w, 1230s, 1176s, 1139w,sh, 1082m, 964w, 937w, 916w, 608w, 748m, 723m, 673m, 636w, 608w, 506m, 482w, 468m. Raman: 2085s, 2062vw, 1569m, 1483w, 1445m, 1381s, 1346m, 1178w, 1138vw, 1087w, 838vw, 750w, 725vw, 646ms, 507vw, 484vw, 296w, 255w,sh, 240w, 206w,sh,br, 166m,br, 116s, 80s.

*Bis[1,3-dimethyl-2(3H)-imidazolethione]di-N-thiocyanatolead(II)*

IR (Nujol mull): 2059s, 1566m, 1343w, 1231m, 1174m, 1082w, 749w, 726m, 672m, 633w, 504w, 462vw. Raman: 2061s, 2036w, 1567w, 1433m, 1393m, 1177w, 1137vw, 1086vw, 748vw, 675w, 639w, 505w, 455vw, 297vw, 260w,sh, 254w, 181w,sh,br, 156m,sh,br, 127s,br, 110m,sh, 80m.

*X-ray crystallographic data*

Suitable crystals of both $Pb(NCS)_2(dmit)_2$ and $Cd(NCS)_2(dmit)_2$ were mounted on a glass fiber using epoxy cement such that the longest crystal dimension was approximately parallel to the fiber axis. Unit cell parameters were determined on a Syntex $P2_1$ four circle diffractometer equipped with a graphite monochromator (Bragg $2\theta$ angle = 12.2°) using Mo K$\alpha$ ($\lambda$ = 0.71069 Å) radiation at a take-off angle of 6.75°. Fifteen reflections were machine centered and used in least-squares refinement of the lattice parameters. Omega scans of several low $2\theta$ angle reflections gave peak widths at half-height of less than 0.24 Å indicating a satisfactory mosaic spread for the crystal examined. Axial photographs were used to determine the space group with zero and upper level intensity data being examined for systematic absences in the usual fashion.

Intensity data were collected using $\omega$ scans with X-ray source and monochromator settings identical to those used for determination of the unit cell parameters. A variable scan rate of 3.91 to 29.3° $min^{-1}$ was used, and a scan width of 1.0° was sufficient to collect all the peak intensity. Stationary background counts were measured at the beginning and at the end of each scan with a total background-to-scan time ratio of 1.0. No significant fluctuations were observed in the intensities of three standard reflections measured every 100 reflections. Intensities were calculated from the total scan count and background counts by the usual relationship.

The intensities were assigned standard deviations in the usual manner, and intensity data are summarized for the two compounds in Table 1. Reflections were collected in a complete quadrant ($\pm h+k+l$) out to $2\theta = 50°$. Reflections were accepted as statistically above background on the basis of $F$ being greater than $2.5\sigma(F)$. Lorentz and polarization corrections were made in the usual way. Absorption corrections were not applied.

*Solution and refinement of the structure*

Computations were performed using the standard programs [9], and were carried out on the CDC Cyber 74 System. For structure factor calculations, the scattering factors were taken from the International Tables for X-Ray Crystallography [10]. The agreement factors are defined in the conventional way. In all least-squares refinements, the quantity minimized has been previously defined [11]. The weighting scheme based on counting statistics are also as previously defined for the calculation of $R_w$ and in least-squares refinement [11].

The structure was solved using a Patterson map. Hydrogen atoms were not added. Final calculated values for $R$ and $R_w$ as well as other crystallographic data for both compounds are summarized in Table 1. Table 2 lists final positional parameters for the non-hydrogen atoms, calculated hydrogen positions and isothermal parameters. Interatomic angles and distances for the metal coordination sphere and for the ligands are listed in Tables 3 and 4, respectively. See also 'Supplementary material'.

TABLE 1. Data collection and processing parameters

| | | |
|---|---|---|
| Molecular formula | $C_{12}H_{16}N_4PbS_4$ | $C_{12}H_{16}N_4CdS_4$ |
| Molecular weight | 551.54 | 484.77 |
| Unit cell parameters | | |
| $a$ (Å) | 11.118(2) | 10.911(2) |
| $b$ (Å) | 14.121(4) | 14.172(2) |
| $c$ (Å) | 12.970(3) | 12.471(2) |
| $\beta$ (°) | 108.29(2) | 107.54(1) |
| $V$ (Å$^3$) | 1933.4 | 1838.7 |
| $Z$ | 4 | 4 |
| $F(000)$ | 1048 | 968 |
| Density (calc.) (g/cm$^3$) | 1.895 | 1.752 |
| Density (obs.) (g/cm$^3$) | 1.93 | 1.75 |
| Space group | $C2/c$ | $C2/c$ |
| Crystal size (mm) | 0.48×0.17×0.12 | 0.41×0.34×0.31 |
| Unique data measured | 1708 | 1617 |
| Observed data with $\|F_o\| > 2.5\sigma\|F_o\|$ | 1487 | 1524 |
| Conventional $R$ | 0.030 | 0.031 |
| Weighted $R$ | 0.030 | 0.038 |

## Results and discussion

*Solution state data*

Solution data in dimethylformamide (DMF) summarized previously for $Pb(NCS)_2(dmit)_2$ indicated that the complex was dissociated in solution, and that the dissociation was both ionic and molecular [1]. Although molecular weight was not determined for $Cd(NCS)_2(dmit)_2$, specific conductivity in $CH_3CN$ indicated this compound to be a non-electrolyte, and the relative shift of the methyl protons in the NMR spectrum were virtually identical to that of uncomplexed dmit ($\delta$ 3.51) [12] indicating molecular dissociation similar to that noted for $CdCl_2(dmit)_2$ [13].

*Crystallographic data*

The principle structure about the metal coordination sphere for both $Pb(NCS)_2(dmit)_2$ and $Cd(NCS)_2(dmit)_2$ is seen in Fig. 2. The primary structural result of this study is similar to that noted earlier for the mono-oxalato complexes of Pb(II) and Cd(II) [5], viz. that

TABLE 2. Atomic parameters $x$, $y$, $z$ ($\times 10^4$) and isotropic temperature factors ($B_{iso}$) for (a) $Cd(NCS)_2(dmit)_2$ and (b) $Pb(NCS)_2(dmit)_2$ (e.s.d.s given in parentheses.)

| | $x$ | $y$ | $z$ | $B_{iso}$ |
|---|---|---|---|---|
| (a) | | | | |
| Cd | 0 | 204(1) | 1/4 | 2.56(2) |
| S1 | 2531(1) | 15(1) | 3060(1) | 3.08(4) |
| S2 | −141(1) | 1688(1) | 938(1) | 3.24(5) |
| N1 | 3442(3) | 344(3) | 1284(3) | 2.96(14) |
| N2 | 3162(3) | 1619(3) | 2124(3) | 3.03(14) |
| N3 | −248(3) | −828(3) | 954(3) | 3.27(16) |
| C1 | 3044(3) | 675(3) | 2136(3) | 2.50(15) |
| C2 | 3796(4) | 1092(3) | 724(4) | 3.86(19) |
| C3 | 3617(4) | 1877(3) | 1243(4) | 3.98(20) |
| C4 | 3496(5) | −658(3) | 1003(4) | 4.18(22) |
| C5 | 2881(5) | 2272(3) | 2922(5) | 4.51(24) |
| C6 | 101(3) | 1158(3) | −157(3) | 2.41(15) |
| HC2 | 4100 | 960 | 60 | 4(1) |
| HC3 | 3660 | 2560 | 1040 | 5(2) |
| HC4A | 3200 | −1060 | 1480 | 12(3) |
| HC4B | 3880 | −810 | 330 | 12(3) |
| HC4C | 4400 | −700 | 1450 | 19(4) |
| HC5A | 3370 | 2900 | 2940 | 7(2) |
| HC5B | 2010 | 2340 | 2810 | 9(2) |
| HC5C | 3270 | 1950 | 3660 | 19(4) |
| (b) | | | | |
| Pb | 0 | 236(1) | 1/4 | 3.02(2) |
| S1 | 2742(2) | −105(2) | 3050(2) | 3.86(9) |
| S2 | 149(3) | −1829(2) | −829(2) | 5.09(11) |
| N1 | 3470(5) | 324(4) | 1280(4) | 3.4(3) |
| N2 | 3203(5) | 1559(4) | 2163(4) | 3.5(3) |
| N3 | −366(7) | −870(5) | 870(6) | 5.4(4) |
| C1 | 3135(6) | 614(5) | 2154(5) | 3.0(3) |
| C2 | 3735(7) | 1105(6) | 743(6) | 4.4(4) |
| C3 | 3569(7) | 1874(6) | 1293(6) | 4.4(4) |
| C4 | 3536(9) | −667(7) | 970(7) | 5.3(5) |
| C5 | 2935(9) | 2171(6) | 2979(7) | 5.2(4) |
| C6 | −152(7) | −1248(5) | 160(6) | 3.7(4) |
| HC2 | 4380 | 940 | 130 | 7(3) |
| HC3 | 3790 | 2580 | 1150 | 4(2) |
| HC4A | 4500 | −1030 | 1720 | 17(5) |
| HC4B | 3700 | −730 | 190 | 18(6) |
| HC4C | 2680 | −1060 | 930 | 26(9) |
| HC5A | 2370 | 1730 | 3440 | 15(5) |
| HC5B | 2350 | 2770 | 2580 | 18(7) |
| HC5C | 3800 | 3440 | 3540 | 22(8) |

the two dmit complexes are not only isomorphous but isostructural as well. Apart from expected differences in metal–ligand bond distances and minor differences in angles as seen in Table 3, the structures for both complexes are best described as isostructural polymers comprised of zigzag chains of $MS_4N_2$ distorted octahedra sharing common edges through almost perfectly linear bridging SCN groups displaced *cis* to each other relative to the central metal atom. Thiourea ligands are displaced *trans* to each other and the ring plane is almost parallel to the thiocyanate–metal plane. Figure 3 shows two stick-drawing perspectives of the polymeric chain along

TABLE 3. Selected metal–ligand interatomic distances (Å) and angles (°) with e.s.d.s given in parentheses (see Fig. 1)

| | $Pb(NCS)_2(dmit)_2$ | $Cd(NCS)_2(dmit)_2$ | $Cd(NCS)_2(etu)_2$[a] |
|---|---|---|---|
| M–S1(S1′) | 2.945(2) | 2.650(1) | 2.60(1) |
| M–S2(S2′) | 3.092(3) | 2.839(1) | 2.73(2) |
| M–N3(N3′) | 2.557(7) | 2.370(3) | 2.53(13) |
| S1–M–S1′ | 161.2(1) | 168.4(1) | NR |
| S1–M–S2<br>S1′–M–S2′ | 97.2(1) | 95.3(1) | 93.2(5) |
| S1–M–S2′<br>S1′–M–S2 | 96.5(1) | 93.3(1) | 83.7(5) |
| S1–M–N3<br>S1′–M–N3′ | 79.4(2) | 82.5(1) | 88.5(8) |
| S1–M–N3′<br>S1′–M–N3 | 89.1(2) | 90.4(1) | 95.0(8) |
| S2–M–N3′<br>S2′–M–N3 | 84.6(2) | 85.9(1) | 93.2(26) |
| S2–M–S2′ | 86.7(1) | 84.5(1) | 95.1(8) |
| N3–M–N3′ | 104.7(3) | 103.8(2) | 78.4(59) |
| S2–M–N3<br>S2′–M–N3′ | 169.7(2) | 170.0(2) | NR |
| M–S1–C1 | 101.8(3) | 107.2(2) | 111.6(11) |
| M–S2–C6 | 101.8(2) | 104.0(2) | 109.1(44) |
| M–N3–C6 | 157.6(6) | 160.2(3) | 143(12) |

[a]Ref. 4. Numbering system altered from original paper to match analogous bonds in this study. NR = value not reported.

TABLE 4. Selected ligand interatomic distances (Å) and angles (°) with e.s.d.s given in parentheses

| | $Pb(NCS)_2(dmit)_2$ | $Cd(NCS)_2(dmit)_2$ |
|---|---|---|
| dmit | | |
| C1–S1 | 1.700(7) | 1.705(4) |
| C1–N1 | 1.362(8) | 1.348(5) |
| C1–N2 | 1.336(9) | 1.345(5) |
| N1–C2 | 1.384(9) | 1.386(5) |
| N1–C4 | 1.465(5) | 1.468(5) |
| N2–C3 | 1.387(9) | 1.385(5) |
| N2–C5 | 1.468(10) | 1.456(6) |
| C2–C3 | 1.343(12) | 1.331(7) |
| C1–N1–C2 | 109.7(6) | 109.6(3) |
| C1–N1–C4 | 124.4(6) | 124.8(3) |
| C2–N1–C4 | 125.9(6) | 125.6(4) |
| C1–N2–C3 | 110.1(6) | 109.2(3) |
| C3–N2–C5 | 125.1(6) | 125.0(4) |
| C1–N2–C5 | 124.8(6) | 125.7(4) |
| S1–C1–N1 | 125.9(5) | 126.3(3) |
| S1–C1–N2 | 128.0(5) | 127.3(3) |
| N1–C2–C3 | 106.9(6) | 106.9(4) |
| N2–C3–C2 | 107.3(6) | 107.8(4) |
| N1–C1–N2 | 106.1(6) | 106.4(3) |
| SCN | | |
| C6–N3 | 1.152(10) | 1.153(5) |
| C6–S2 | 1.643(8) | 1.647(4) |
| S2–C6–N3 | 177.6(7) | 176.6(3) |

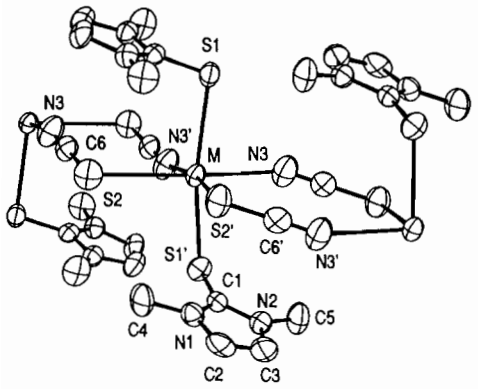


Fig. 2. ORTEP drawing of coordination sphere for metal; M = Cd, Pb. Thermal ellipsoids are drawn at the 50% probability level.

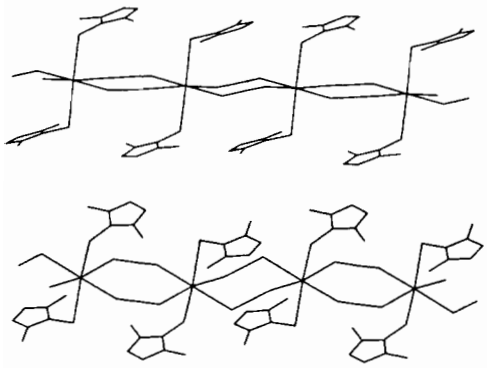

Fig. 3. Stick drawings showing two different perspectives of the polymeric chain along *c* axis.

the *c* axis and the relative disposition of the ligand rings. Comparing bond distances with known values of covalent radii sums for the metal–thiocyanate (N– and S–) bonds justifies the N-bonded formulation for these complexes. The bond angles in the lead complex show slightly greater deviations from 90° ranging from 79.37 to 104.66° whereas the cadmium complex has angles ranging from 82.46 to 103.79°. The maxima and minima are analogous angles in both complexes, however, (max. N3–M–N3′ and min. S1–M–N3), and from careful inspection of Table 3 it can be seen that the similar relative modes of deviation from the idealized 90° exist within the coordination spheres of both metals. Table 5 shows computed non-bonded S···S, S···N and N···N contacts in the coordination sphere of each metal and compares them to the expected van der Waals sum. Also included in Table 5 are relevant computed non-bonded contacts taken from data reported for the structure of $Pb(NCS)_2(dmso)_2$ [3] and $Cd(NCS)_2(etu)_2$ [4].

In comparing the structures $Cd(NCS)_2(etu)_2$ and $Cd(NCS)_2(dmit)_2$, there appear to be significant differences. As seen in Table 3, the main significant difference in bond distances is seen in the Cd–S2(S2′) bonds with the dmit complex having the longer contact (2.839 versus 2.73 Å). Bond angle differences are not large, but the pattern of distortion is distinctly different as seen in both Tables 3 and 5. The greatest deviation from 90° in the dmit complex is observed in the N3–Cd–N3′ angle (103.8°) as noted earlier, whereas in the etu complex this angle shows the greatest deviation in the opposite direction (78.4°). The N···N contact is consequently closer to the expected van der Waals contact (3.10 Å) in the etu complex than in the dmit complex. Table 5 also shows the S···S non-bonding contacts to be longer in the dmit complex whereas in the etu complex, with the exception of the thiocyanate-S contact (4.03 Å), the values are closer to the expected van der Waals contacts. The S···N contacts are in general comparable, but the patterns for distortion are distinctly different in the two complexes. This may be due in part to the disposition of the ligand ring relative to the metal–thiocyanate plane. As mentioned above, in the dmit complex, the ring is almost parallel to the metal–thiocyanate plane whereas in the etu complex, it is almost perpendicular though canted in the direction which allows what appears to be hydrogen bonding between the hydrogen attached to the nitrogen of the ligand and the thiocyanate nitrogen [4]. Thus, some of the differences, especially the greater non-bonded contacts and/or differences in angles may be attributed to the more intense ligand–ligand repulsions in the dmit complex. Inspection of Figs. 2 and 3 show that one of the methyl groups (C5) is displaced in the direction of the thiourea sulfur on a neighboring ligand thus possibly causing a greater opening of the N–Cd–N

TABLE 5. Non-bonding contacts (Å) in coordination sphere of related Pb(II) and Cd(II) complexes

| | $Pb(NCS)_2(dmit)_2$ | $Cd(NCs)_2(dmit)_2$ | $Cd(NCS)_2(etu)_2$[a] | $Pb(NCS)_2(dmso)_2$[b] | VDW[c] |
|---|---|---|---|---|---|
| S1···S2<br>S1′···S2′ | 4.53 | 4.05 | 3.87 | | |
| S1···S2′<br>S1′···S2 | 4.50 | 3.99 | 3.56 | | |
| S2···S2′ | 4.24 | 3.82 | 4.03 | 5.57 | 3.60 |
| S1···N3<br>S1′···N3′ | 3.52 | 3.32 | 3.78 | | |
| S1···N3′<br>S1′···N3 | 3.87 | 3.82 | 3.58 | | |
| S2···N3′<br>S2′···N3 | 3.83 | 3.57 | 3.82 | 3.69[d]<br>3.59[d] | 3.35 |
| N3···N3′ | 4.04 | 3.73 | 3.20 | 3.14 | 3.10 |

[a]Ref. 4. Numbering system altered from original papter to match analogous bonds in this study. [b]Ref. 3. Numbering system altered from original paper to match analogous bonds in this study. [c]van der Waal's radii sum computed from data listed in ref. 14. [d]Arbitrarily chosen with regard to numbering system since symmetry requirements differ for this complex.

angle and subsequent greater N···N non-bonding contact. This may also explain why the S1–Cd–S1′ bond is non-linear (168.4°) and displaced in such a way so as to open up the S···S contacts and tighten down some of the S···N contacts relative to the expected van der Waals values in the dmit complex.

As stated earlier, the principle reason for the above comparison is to provide information concerning the pattern of distortion in the absence of a lone-pair of electrons in the valence shell such as would be expected for the Pb(II) complex. As can be seen from Tables 3 and 5, however, the distortion pattern is identical between the Cd(II) and the Pb(II) dmit complexes. Thus there is no strong evidence for a stereoactive non-bonded electron pair in the coordination sphere of Pb based on similarity of observed distortion patterns. There may be some evidence of lone-pair bonded pair repulsions, however, based on the somewhat expanded S···S contacts over the expected van der Waals values and the even greater deviation from linearity in the S1–Pb–S1′ bond (161.2°). This tends to suggest a lone-pair aimed in the direction of the sulfur atoms in the coordination sphere, but no single S···S non-bonded contact or S–Pb–S bond angle give evidence for the localization point. Ligand steric repulsions cited earlier in the structure of $Cd(NCS)_2(dmit)_2$ may, in part, override lone-pair bonded-pair repulsions as noted by other authors [3, 15–17], but the larger coordination sphere of Pb as reflected in the longer M–N and M–S distances should mitigate some of the ligand–ligand interaction. A possible explanation lies in a theory proposed by Wynne [18] who noted a correlation between the hard–soft acid–base (HSAB) [19] nature of the ligand and the stereoactivity of lone pairs in $AX_6E$ systems. It was proposed that the lone-pair was stereoactive in the presence of hard donor sites where the interaction with the acceptor site is more ionic in nature, but inactive in the presence of soft bases which have low-lying empty orbitals which could partially delocalize the lone-pair. Several examples were cited in support of this argument. An example of mixed hard–soft donor sites was reported by Barayni *et al.* [3] with the structure of $Pb(NCS)_2(dmso)_2$ which has a highly distorted octahedral coordination sphere about the lead atom. Table 5 includes the S···S non-bonded contact for $Pb(NCS)_2(dmso)_2$ since there is evidence for a stereoactive lone-pair in the coordination sphere of Pb directed toward the Pb–S bonds which are also notably longer (3.19 Å) than those reported for this structure (3.092 Å) [3]. Table 5 shows the evidence for the stereoactive lone-pair with the S···S non-bonded contact computed by us to be 5.57 Å, much larger than the expected sum of the van der Waals radii, and much larger than the originally reported 4.74 Å which we believe to be in error since our calculations concur with the all of the other non-bonded contacts reported by the authors [3]. This even larger opening along with the non-linear O–Pb–O bond (160.1°) gives more weight to the argument for a stereoactive lone-pair of electrons displaced toward the S···S non-bonded edge. In the case of $Pb(NCS)_2(dmso)_2$, there is a preponderance of hard donors (O and N) which may force the lone pair toward the softer sites (S) whereas in the case of the dmit complex, the majority of donor sites are sulfur atoms thus allowing at least partial delocalization of the lone pair and reducing lone-pair bonded-pair repulsions. Thus a combination of partial delocalization by soft donors and ligand steric constraints may constitute a reasonable explanation for what appears to be lone-pair stereoinactivity in the valence shell of lead in $Pb(NCS)_2(dmit)_2$.

Thiocyanate groups were essentially linear, and C–S and C–N distances are similar to those noted by others for bridging SCN moieties [3, 4, 20–22]. Bond distances and angles for dmit compare favorably to those noted for the coordinated ligand in other studies [14, 23].

*Solid state vibrational data*

The region of principle interest for these complexes lies below 2100 $cm^{-1}$. Very strong thiocyanate C–N stretches are noted in the IR spectra (with corresponding peaks in the Raman) at 2086 and 2059 $cm^{-1}$ for the Cd(II) and Pb(II) complexes, respectively. These fall in and near the range noted by Baranyi *et al.* for bridging thiocyanate moieties (2165–2065 $cm^{-1}$) [24]. The thiocyanate C–S modes are assigned to the peaks around 749 $cm^{-1}$ in both the Raman and IR spectra, again similar to those noted by Baranyi *et al.* (800–750 $cm^{-1}$) [24] and Czakis-Sulikowska and Kusnik [25] for bridging SCN groups.

Metal–nitrogen modes and metal–sulfur modes are observed for both complexes in the Raman below 400 $cm^{-1}$. Peaks from *c.* 300 to 240 $cm^{-1}$ are ligand modes associated with dmit and are observed in spectra from this study as well as in other Raman spectra recorded for other main group metal halide dmit complexes [26]. Strong peaks from 116 $cm^{-1}$ down to 50 $cm^{-1}$ are also observed in both spectra and appear to be associated with dmit as well [26]. Thus, in the Cd(II) complex there are two peaks that may be associated with the Cd–N and Cd–S modes – 206 and 166 $cm^{-1}$. Goel [27] reports the solid state vibrational spectra for $Cd(NCS)_2$ and from the known centrosymmetric $D_{4h}$ site symmetry [28] of this complex assigns asymmetric and symmetric Cd-N stretches to peaks at 204 and 198 $cm^{-1}$, respectively. Similarly, the Cd–S modes are assigned to peaks at 140 $cm^{-1}$ in the far-IR and 158 and 131 $cm^{-1}$ in the Raman. Persson *et al.* make a similar assignment for Cd–N in the Raman spectrum (202 $cm^{-1}$) [28]. Based on the similarity of frequencies,

the band at 206 $cm^{-1}$ is assigned as the Cd–N stretch and the one at 166 $cm^{-1}$ as the Cd–S stretch for $Cd(NCS)_2(dmit)_2$. There is a great deal of similarity in this spectrum to that reported by Selvarajan for $Cd(NCS)_2(tu)_2$ which is included in a paper detailing the far-IR and Raman spectra for $MX_2(tu)_2$ where M = Zn and Cd, X = SCN and Cl, and tu = thiourea [29]. The assignments are based on the known tetrahedral structure for $ZnCl_2(tu)_2$. Only two lines are observed for $Cd(NCS)_2(tu)_2$ below 400 $cm^{-1}$ – one at 207 $cm^{-1}$ which is assigned as the Cd–S stretch, and one at 148 $cm^{-1}$ which is assigned as the Cd–N stretch. However, also reported are the C–N and C–S stretches which occur in the Raman at 2058 and 794 $cm^{-1}$, respectively. Based on the ranges reported by Baranyi *et al.* [24] and our own data above, these numbers tend to suggest a bridging SCN group rather than an N-bonded moiety as suggested by the author. Thus the tetrahedral analog may not be valid, and a structure similar to those observed in this study may be indicated. Furthermore, it seems unusual that the Cd–N stretching frequency would be lower than the Cd–S frequency especially in light of the spectra reported above for $Cd(NCS)_2$. A more reasonable assignment based on frequency and structural similarity would be to assign the 207 $cm^{-1}$ peak as the Cd–N stretch and the 148 $cm^{-1}$ peak as the Cd–S stretch.

The assignments for this region in the Raman spectrum of $Pb(NCS)_2(dmit)_2$ are not quite as straightforward. Very little literature precedent is found to aid in the assignments of Pb–N and Pb–S peaks, and the Raman spectrum in this region is essentially one large coalesced peak centered at 127 $cm^{-1}$ with broad shoulders at 156 and 181 $cm^{-1}$. The Raman spectrum for $Pb(NCS)_2$ shows peaks at 186 and 156 $cm^{-1}$ [26] which may be assigned as the Pb–N stretch and the Pb–S stretch, respectively, based on the similarity of structure to $Cd(NCS)_2$ [2]. Support for this also comes from observed far-IR spectra recorded by Adams and Cornell [30] for $Pt(tu)_4(ClO_4)_2$ wherein a broad peak at 161 $cm^{-1}$ is assigned as the Pb–S stretch. The 127 $cm^{-1}$ peak is broad as noted earlier and may be a combination of dmit and lattice modes as well.

## Supplementary material

Final thermal parameters and a list of calculated and observed structure factor tables are available from the author for correspondence on request.

## Acknowledgements

D.J.W. thanks the Kennesaw College Faculty Development Fund and the Wilcom Foundation of Marietta, GA (USA) for partial support of this research. We also thank Dr Martha C. Williams of the Wilcom Foundation for her help in computational programming, and we are grateful to Professor Nai-Teng Yu of Georgia Tech for the use of the FT-Raman spectrophotometer.

## References

1 D. J. Williams, R. L. Jones and P. H. Poor, *Inorg. Chim. Acta, 144* (1988) 237.
2 J. A. A. Mokuolo and J. C. Speakman, *Acta Crystallogr., Sect. B, 31* (1975) 172.
3 A. D. Baranyi, M. Onyszchuk, S. Fortier and G. Donnay, *J. Chem. Soc., Dalton Trans.*, (1976) 2301.
4 L. Cavalca, M. Nardelli and G. Fava, *Acta Crystallogr., 13* (1960) 125.
5 H. Sheng-Hua, W. Ru-Ji and T. C. W. Mak, *J. Crystallogr. Spectrosc. Res., 20* (1990) 99.
6 D. J. Williams, B. Rubin, J. Epstein, W. K. Dean and A. Viehbeck, *Cryst. Struct. Commun., 11* (1982) 1.
7 L. P. Battaglia, A. Bonamartini Corradi, M. Nardelli and M. E. Vidoni Tani, *J. Chem. Soc., Dalton Trans.*, (1978) 583.
8 B. L. Benac, E. M. Burgess and A. J. Arduengo III, *Org. Synth., 64* (1986) 92.
9 E. J. Gabe, F. L. Lee and Y. Le Page, in G. M. Sheldrick, C. Kruger and R. Goddard (eds.), *Crystallographic Computing 3: Data Collection, Structure Determination, Proteins, and Databases,* Clarendon, Oxford, 1985, pp. 167–174.
10 *International Tables for X-Ray Crystallography,* Vol. IV, Kynoch, Birmingham, UK, 1974.
11 D. J. Williams, G. Ramirez and D. VanDerveer, *J. Crystallogr. Spectros. Res., 16* (1986) 309.
12 D. J. Williams and K. J. Wynne, *Inorg. Chem., 17* (1978) 1108.
13 D. J. Williams, P. H. Poor, G. Ramirez and B. L. Heyl, *Inorg. Chim. Acta, 147* (1988) 221.
14 J. E. Huheey, *Inorganic Chemistry,* Harper and Row, New York, 3rd edn., 1983, p. 258.
15 R. J. Gillespie, *Molecular Geometry,* Van Nostrand, London, 1972, p. 71.
16 S. L. Lawton, C. J. Fuhrmeister, R. G. Haas, C. S. Jarman, Jr. and F. G. Lohmeyer, *Inorg. Chem., 13* (1974) 135.
17 D. J. Williams, C. O. Quicksall and K. M. Barkigia, *Inorg. Chem., 21* (1982) 2097.
18 K. J. Wynne, *J. Chem. Educ., 50* (1973) 328.
19 R. G. Pearson, *Chem. Brit., 3* (1967) 103.
20 M. Cannas, G. Carta, A. Cristini and G. Marongiu, *J. Chem. Soc., Dalton Trans.*, (1976) 301.
21 N. Bertazzi, G. Alonzo, L. P. Battaglia, A. Bonarmatini Corradi and G. Pelosi, *J. Chem. Soc., Dalton Trans.*, (1990) 2403.
22 L. M. Engelhardt, B. M. Furphy, J. McB. Harrowfield, J. M. Patrick, B. W. Skelton and A. H. White, *J. Chem. Soc., Dalton Trans.*, (1989) 595.
23 F. M. Freeman, J. W. Ziller, H. N. Po and M. C. Keindl, *J. Am. Chem. Soc., 110* (1988) 2586.
24 A. D. Baranyi, R. Makhija and M. Onyszchuk, *Can. J. Chem., 54* (1976) 1189.
25 D. M. Czakis-Sulikowska and B. Kusnik, *Rocz. Chem., 43* (1969) 1363.
26 D. J. Williams and L. A. Lipscomb, unpublished data.
27 R. G. Goel, *Spectrochim. Acta, Part A, 37* (1981) 557.
28 I. Persson, A. Iverfeldt and S. Arhland, *Acta Chem. Scand., 35* (1981) 295.
29 A. Selvarajan, *Indian J. Pure Appl. Phys., 8* (1970) 338.
30 D. M. Adams and J. B. Cornell, *J. Chem. Soc. A,* (1967) 884.